



## Fabrication and nanoindentation properties of TiN/NiTi thin films and their applications in electrochemical sensing

Ashvani Kumar<sup>a</sup>, Devendra Singh<sup>b</sup>, Rajendra N. Goyal<sup>c,\*</sup>, Davinder Kaur<sup>a</sup>

<sup>a</sup> Department of Physics and Center of Nanotechnology, Indian Institute of Technology Roorkee, Roorkee 247667, India

<sup>b</sup> Metallurgy and Materials Engineering Department, Indian Institute of Technology Roorkee, Roorkee 247667, India

<sup>c</sup> Department of Chemistry, Indian Institute of Technology Roorkee, Roorkee 247667, India

### ARTICLE INFO

#### Article history:

Received 13 October 2008

Received in revised form 5 January 2009

Accepted 5 January 2009

Available online 20 January 2009

#### Keywords:

TiN/NiTi heterostructures

Nanoindentation

Sensors

Corrosion resistance

### ABSTRACT

Nanocrystalline TiN/NiTi thin films have been grown on silicon substrate by dc magnetron sputtering to improve the corrosion and mechanical properties of NiTi based shape memory alloys without sacrificing the phase transformation effect. Interestingly, the preferential orientation of the TiN films was observed to change from (1 1 1) to (2 0 0) with change in nature of sputtering gas from 70% Ar + 30% N<sub>2</sub> to 100% N<sub>2</sub>. In present study the influence of crystallographic orientation of TiN on mechanical and corrosion properties of TiN/NiTi thin films was investigated. TiN (2 0 0)/NiTi films were found to exhibit high hardness, high elastic modulus, and thereby better wear resistance as compared to pure NiTi and TiN (1 1 1)/NiTi films. Electrochemical test revealed that TiN coated NiTi film exhibits better corrosion resistance in 1 M NaCl solution as compared to uncoated NiTi film. The application of TiN/NiTi films in the electrochemical sensing of dopamine, which has a critical physiological importance in Parkinson's disease, has been demonstrated. A comparison of voltammetric response of dopamine at silicon based electrodes modified with different nanocrystalline coatings indicated that these films catalyze the oxidation of dopamine.

© 2009 Elsevier B.V. All rights reserved.

### 1. Introduction

It has been demonstrated that NiTi shape memory alloy (SMA) thin films are promising materials to fabricate micro devices for micro-electro-mechanical systems (MEMS) and bio-MEMS such as micropumps, microwrappers and stents for neurovascular blood vessels [1–3]. However, there are still some concerns for the wide application of SMA thin films because of their unsatisfactory mechanical and tribological performances, chemical resistance and biological reliability. High nickel content in NiTi alloys often stimulated suspicion for their medical use because of nickel toxicity [4,5]. The limited hardness and wear resistance of NiTi make it difficult to be used in orthodontic and MEMS applications. In order to improve surface properties, corrosion resistance and suppression of Ni ions release of NiTi shape memory alloys, many techniques such as nitrogen ion implantation [6], laser surface treatment [7], thermal and anodic oxidation [8,9], have been employed. The problems of these surface treatments are high cost, possible surface or ion induced damage, amorphous phase formation, or degradation of shape memory effects. The magnetron sputtering has important specific advantages such as low levels of impurities and easy control of the deposition rate and also enables the production of

thin films of various morphology and crystallographic structure. The deposition of nanocrystalline and nanocomposite thin films via magnetron sputtering has been reported in literature [10,11].

The present study explored the insitu deposition of hard and adherent nanocrystalline titanium nitride (TiN) protective coating on NiTi thin films by dc magnetron sputtering. TiN is chosen for passivation layer due to its superior mechanical properties, excellent corrosion, wear resistance and good biocompatibility and TiN coatings are often used to modify the orthopedic implant materials to extend their life span [12,13]. The purpose of the present study is to examine the effect of crystallographic orientation of TiN on mechanical and corrosion properties of TiN/NiTi heterostructure thin films. The investigation revealed better mechanical and corrosion properties in case of TiN (2 0 0)/NiTi films as compared to TiN (1 1 1)/NiTi and pure NiTi films. The present study also explores the utility of TiN (2 0 0), TiN (2 0 0)/NiTi, TiN (1 1 1)/NiTi nanocrystalline coatings over Si (1 0 0) substrate as working electrode material for electroanalytical purpose.

In recent years the electrodes modified with various nanomaterials have been used for the electrochemical sensing of biologically important compounds as the surface modification has been found to exhibit electrocatalytic effect [14–18]. As electrochemical methods have distinct advantages [19,20] over other conventional methods for determination of dopamine (DA), a catecholamine neurotransmitter generated in various parts of central and peripheral nervous system, hence, careful monitoring of dopamine

\* Corresponding author. Tel.: +91 1332 285794.

E-mail address: [rngcyfcy@iitr.ernet.in](mailto:rngcyfcy@iitr.ernet.in) (R.N. Goyal).

concentration is considered necessary. Parkinson's disease, associated with tremor, rigidity, bradykinesia and postural instability, is one of the most dreadful neurodegenerative disorders of central nervous system (CNS). The disease occurs when dopaminergic neurons decrease or malfunction which is accompanied by a sharp decline in dopamine level [21,22]. Therefore, in the present investigation, the prepared nanocrystalline thin films have been tested for first time as working electrode for dopamine sensing.

## 2. Experimental

Pure NiTi and TiN/NiTi thin films were deposited on (100) silicon substrate of dimensions 1.5 cm × 2 cm by dc magnetron sputtering system (Excel Instruments). High purity (99.99%) titanium and nickel metal targets of 50 mm diameter and 3 mm thickness were used. Substrate holder was rotated at 20 rpm in a horizontal plane to achieve a uniform film composition. All the NiTi films of approximately 2 μm thickness were prepared at substrate temperature of 823 K in an argon (99.99% pure) atmosphere. The target to substrate distance was fixed at approximately 5 cm. No postannealing was performed after deposition. For the deposition of TiN passivation layer, two different sputtering gas mixtures were used: 70% Ar + 30% N<sub>2</sub> (referred henceforth as Ar + N<sub>2</sub>); and 100% N<sub>2</sub>.

The orientation and crystallinity of the films were studied using a Bruker advanced diffractometer of CuKα (1.54 Å) radiations in  $\theta$ -2 $\theta$  geometry at a scan speed of 1°/min. X-ray diffraction (XRD) studies revealed that the NiTi film exhibits austenite phase with (1 1 0) reflection at room temperature and the orientation of protective TiN layer was found to change from (1 1 1) to (2 0 0) with change in sputtering gas from 70% Ar + 30% N<sub>2</sub> to 100% N<sub>2</sub>. The surface morphology of these films was studied using field emission scanning electron microscope (FEI Quanta 200F) and atomic force microscope (NT-MDT: NTEGRA Model). The film thickness was measured using a surface profilometer and cross sectional field emission scanning electron microscopy (FESEM). The resistivity of the films was measured by a four probe resistivity method using a liquid nitrogen cryocooler and Keithley instruments over a temperature range 90–450 K. The values of martensite start temperature and austenite final temperature were found to be 290 K, 320 K for pure NiTi; 260 K, 326 K for TiN (1 1 1)/NiTi and 242 K, 326 K for TiN (2 0 0)/NiTi films, respectively.

A Hysitron Triboindenter was used to perform nanoindentation tests. Sixteen nanoindentation tests were performed on each sample using a diamond Berkovich indenter probe to determine the hardness and reduced modulus. Each test consisted of a 5-s linear loading segment to a peak load, followed by a 2-s holding segment at the peak load, and finally a 5-s linear unloading segment. The testing temperatures were 298 K, 323 K and 380 K. The maximum load was set at 5 mN.

The electrochemical experiments were performed with BAS (Bioanalytical Systems, West Lafayette, IN, USA) CV-50W Voltammetric analyzer. A conventional three electrode glass cell was used with a platinum wire as an auxiliary electrode, Ag/AgCl electrode as reference (model MF-2052 RB-5B) and TiN or TiN/NiTi coated silicon as working electrodes. The nanocrystalline thin film deposited on silicon substrate was connected to a thin copper strip (5 mm × 60 mm) and molded between two pieces of scotch tape of size 50 mm × 18 mm. One side of the tape was punched for 3 mm diameter hole to provide the contact of films with the solution. The electrode was then ready for use and was kept in air with contact side upwards. All measurements were carried out at room temperature. Dopamine was purchased from Sisco Research Laboratory, India. All other reagents used were of analytical grade. All solutions were prepared in double distilled water. Phosphate buffer

**Table 1**

A comparison of hardness and reduced elastic modulus for nanocrystalline thin films at different temperatures.

| Sample           | Temperature (K) | Hardness <sup>a</sup> (GPa) | pcReduced modulus <sup>a</sup> , E <sub>r</sub> (GPa) | H/E <sub>r</sub> <sup>a</sup> |
|------------------|-----------------|-----------------------------|---|-------------------------------|
| NiTi             | 298             | 7.3 ± 0.6                   | 134.8 ± 6.4   | 0.054 ± 0.002                 |
|                  | 323             | 8.0 ± 1.2                   | 123.2 ± 8.9   | 0.065 ± 0.004                 |
|                  | 380             | 7.8 ± 1.1                   | 102.6 ± 7.4   | 0.076 ± 0.004                 |
| TiN (1 1 1)/NiTi | 298             | 5.9 ± 0.7                   | 123.6 ± 8.7   | 0.047 ± 0.003                 |
|                  | 323             | 6.1 ± 0.9                   | 126.1 ± 8.9   | 0.048 ± 0.003                 |
|                  | 380             | 6.6 ± 1.1                   | 128.7 ± 10.3  | 0.051 ± 0.004                 |
| TiN (2 0 0)/NiTi | 298             | 12.0 ± 0.8                  | 139.8 ± 4.0   | 0.086 ± 0.003                 |
|                  | 323             | 12.2 ± 1.0                  | 140.2 ± 7.2   | 0.087 ± 0.004                 |
|                  | 380             | 12.7 ± 0.9                  | 142.6 ± 9.7   | 0.089 ± 0.004                 |

<sup>a</sup> The values are mean ± root mean square deviation (RSD) for  $n = 16$ .

solutions were prepared according to the method of Christian and Purdy [23] and the final pH of the solutions was recorded with the pre-calibrated digital pH meter. Stock solution of DA was prepared in doubly distilled water. Required amount of the stock solution was added to 2 ml of phosphate buffer solution ( $\mu = 1.0$  M, pH 7.2) and the total volume was made to 8.0 ml with double distilled water. The electrochemical measurements were then carried out with voltammetric analyser. Differential pulse voltammetry employed had the following parameters: initial  $E$ : 0 mV, final  $E$ : 750 mV, sweep rate: 20 mV/s, sensitivity: 10 μA/V. The corrosion behaviour of pure NiTi and TiN/NiTi films were recorded in 1 M NaCl solution. Before measurement, each sample was immersed in to the electrolyte for 20 min. The sample area exposed to the electrolyte was 0.0707 cm<sup>2</sup> (3 mm diameter).

## 3. Results and discussion

### 3.1. Structural properties

The surface morphology of the TiN/NiTi films prepared in different gas environment were studied using FESEM and is shown in Fig. 1. Pure NiTi film shows uniform, fine and homogenous microstructures with grain size of 96 nm (Fig. 1(a)). Fig. 1(b) and (c) clearly shows the change in grain morphology from strongly faceted pyramid like grains to nonfaceted spherical grains in case of TiN/NiTi films, with change in crystallographic orientation of TiN from (1 1 1) to (2 0 0). The average surface roughness of the pure NiTi, TiN (1 1 1)/NiTi and TiN (2 0 0)/NiTi was measured using atomic force microscopy (AFM) and found to be 10.84, 7.44 and 4.75 nm, respectively.

### 3.2. Mechanical properties

Fig. 2 shows the normalized indentation load–depth curves for NiTi, TiN (1 1 1)/NiTi, TiN (2 0 0)/NiTi thin films at three different temperatures of 298 K, 323 K and 380 K. Fig. 2(b) and (c) exhibits a deflection in load–displacement curve at the contact depth of ~80 nm (shown by the circle), which could be due to the transition from upper TiN layer to underneath NiTi layer. Hardness, reduced modulus and wear behaviour were evaluated using these curves and are summarized in Table 1. The indentation induced superelastic energy recovery ratio ( $\eta_w$ ) was also calculated using following relation [24]:

$$\eta_w = \frac{W_e}{W_t} = \frac{\int_0^{h_r} F dh}{\int_0^{h_{\max}} F dh}$$

where  $W_e$  is the reversible work and  $W_t$  is the total work done. Superelastic energy recovery ratio at room temperature was found

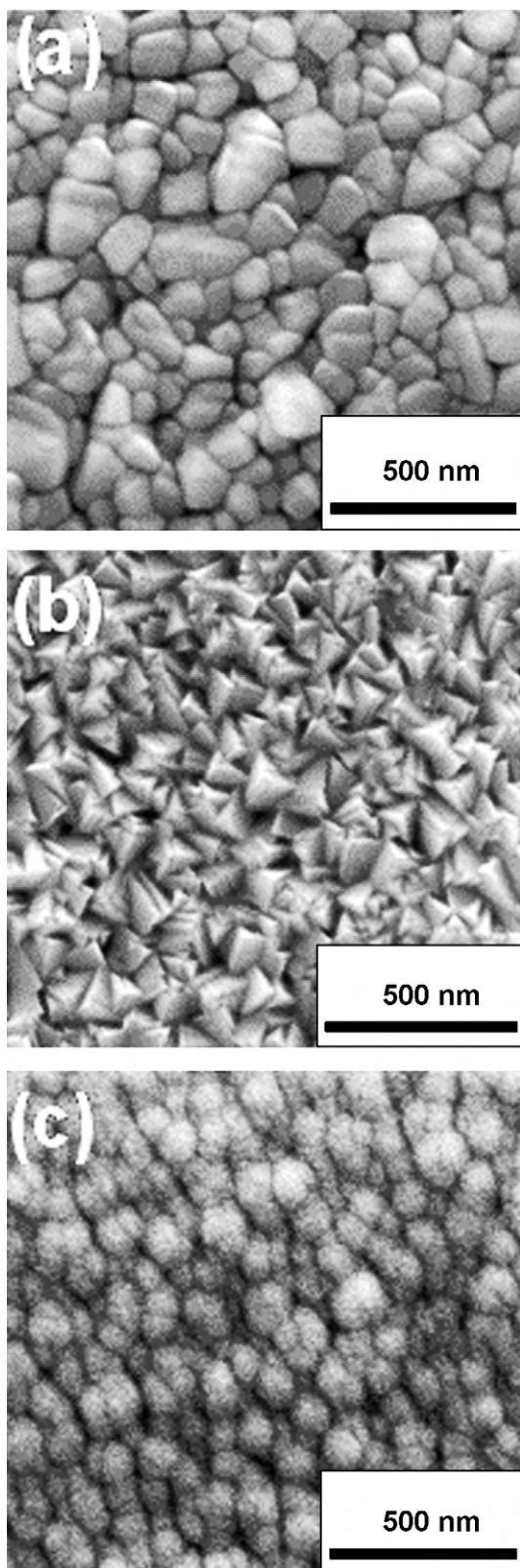


Fig. 1. FESEM images of (a) NiTi film (b) TiN (1 1 1)/NiTi (c) TiN (2 0 0)/NiTi thin films.

to be 0.44, 0.42 and 0.49 for pure NiTi, TiN (1 1 1)/NiTi and TiN (2 0 0)/NiTi films, respectively. Low values of superelastic recovery under Berkovich tip were expected due to the generation of high peak strain levels below the tip that generates high density of dislocations through the conventional plastic deformation. High

dislocation density stabilizes the parent phase and prevents its transformation to martensite thus the high peak strains under a sharp indenting tip inhibit the superelastic recovery. The highest value of indent depth recovery ratio in NiTi using Berkovich indenter has been reported to be 45% at low loads [24]. Inset of Fig. 2 depicts the temperature dependence of superelastic energy recovery ratio ( $\eta_w$ ). It was observed that TiN/NiTi films also exhibit SE energy recovery ratio as comparable to pure NiTi film, which could be due to combined composite properties from top nanocrystalline TiN layer and underneath NiTi layer.

The average hardness ( $H$ ) and reduced elastic modulus ( $E_r$ ) were calculated for each sample from indentation load–depth curves at room temperature and are summarized in Table 1. TiN (2 0 0)/NiTi films were found to exhibit maximum hardness ( $12.0 \pm 0.8$ ) and elastic modulus ( $139.8 \pm 4.0$  GPa). Hardness ( $H$ ) to Young modulus ( $E$ ) ratio has been proposed as the key factor to measure the behaviour of wear resistance of bilayer coatings. It has been reported that the deformation around the indenter surface exhibits piling-up and sinking-in and the tendency of sinking-in increases with increasing  $H/E$  ratio [25]. A relative low value of  $H/E$  ratio (0.054) for pure NiTi films indicate that more fraction of work is consumed in plastic deformation and large plastic strain is expected when contacting a material. In case of TiN (2 0 0)/NiTi film the  $H/E$  ratio (0.086) was found to be higher as compared to NiTi and TiN (1 1 1)/NiTi, which indicate that the TiN (2 0 0) passivated NiTi exhibit better wear resistance.

### 3.3. Electrochemical properties

#### 3.3.1. Voltammetric behaviour of dopamine

It was observed that TiN (2 0 0), TiN (2 0 0)/NiTi and TiN (1 1 1)/NiTi coated silicon electrode exhibit a sharp oxidation peak for dopamine at  $E_p \sim 400$ , 380, and 365 mV, respectively which is much lesser than oxidation peak potential observed at bare silicon (800 mV) as shown in Fig. 3(a) and (b). On the contrary, NiTi coated silicon does not show any oxidation peak for dopamine in the potential range 0–1000 mV (Fig. 3(a)). Since both the TiN/NiTi coated silicon electrodes showed better response for dopamine oxidation, a systematic concentration study of the dopamine was carried out at TiN (2 0 0)/NiTi coated silicon electrode in the concentration range 1–10  $\mu$ M. The peak current as found to increase with the increase in concentration of dopamine is shown in Fig. 4. The linear dependence of peak current on concentration (Fig. 5) can be represented by the relation

$$i_p = 5.059[\text{DA}] + 6.874$$

where  $i_p$  is the current in nA and [DA] is the concentration of dopamine in  $\mu$ M. The correlation coefficient for the linear relation was 0.995. It was observed that TiN/NiTi exhibit dominant catalytic behaviour as compared to TiN/Si film. One of the reasons for this behaviour could be the fact that these films are deposited at high substrate temperature ( $T_s = 823$  K), hence, there are favourable chances of silicon diffusion in TiN film that can be responsible for the suppression of catalytic activity of TiN. While in the case of TiN/NiTi, NiTi is acting as a buffer layer and prevent the silicon diffusion to upper TiN film. Also the calculated value of lattice mismatches for TiN (1 1 1)/NiTi and TiN (2 0 0)/NiTi and was found to be 0.5% and 0.2%, respectively. Therefore, it is concluded that NiTi does not exhibit catalytic activity but acts as a good buffer layer and prevents the silicon diffusion to upper TiN layer.

#### 3.3.2. Interference effect

Biological samples contain many electroactive metabolites, which can interfere in voltammetric determination of any compound. Among these ascorbic acid and uric acid are most

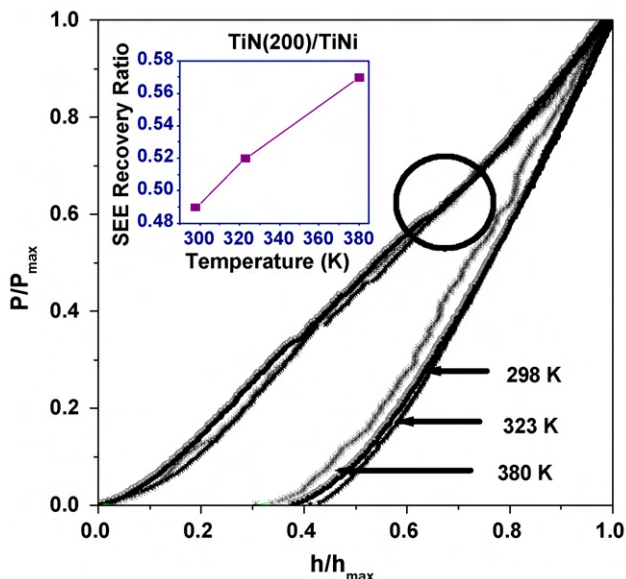
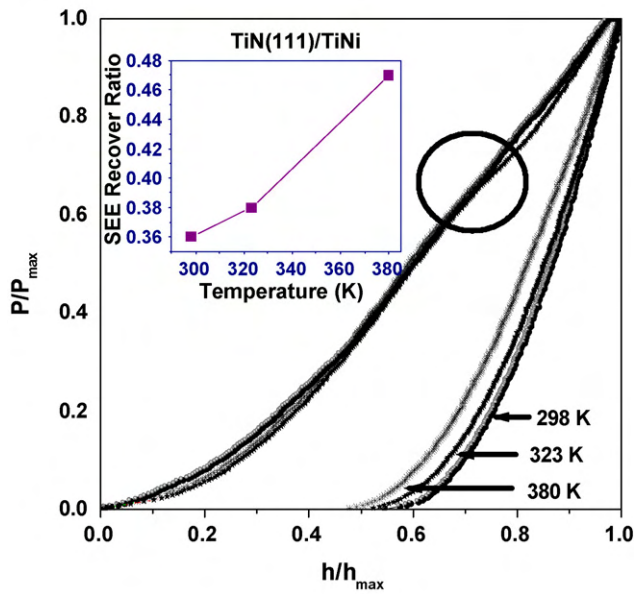
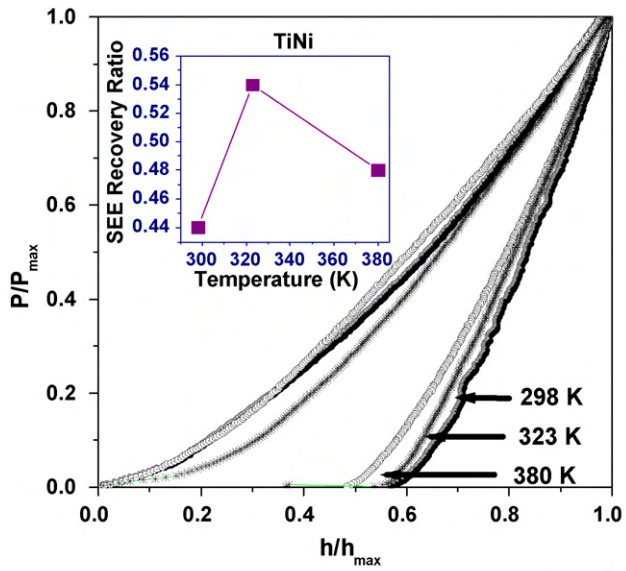


Fig. 2. Normalized indentation load vs. depth curves of (a) NiTi film (b) TiN (111)/NiTi and (c) TiN (200)/NiTi thin films.

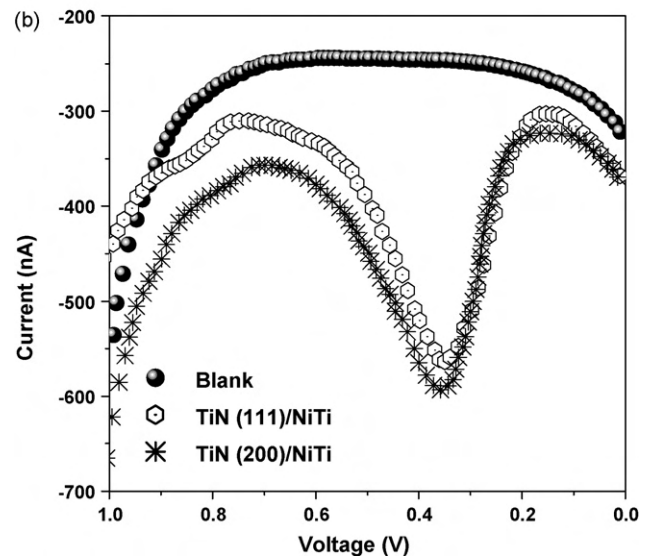
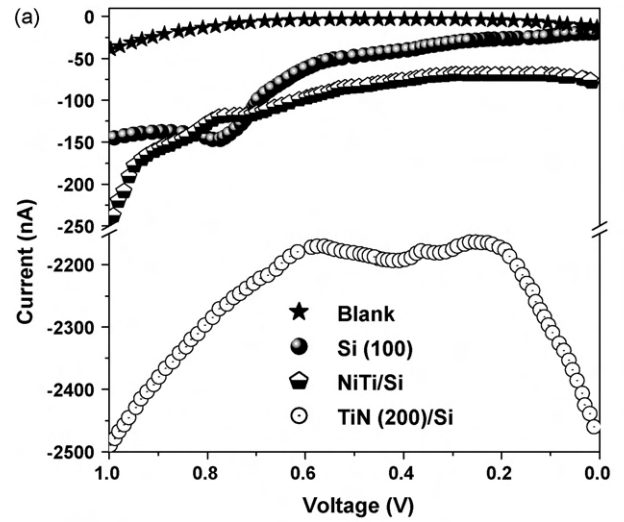


Fig. 3. A comparison of voltammogram of dopamine at pH 7.2 at different working electrodes (a) Si (100), NiTi and TiN (200); (b) TiN (111)/NiTi and TiN (200)/NiTi.

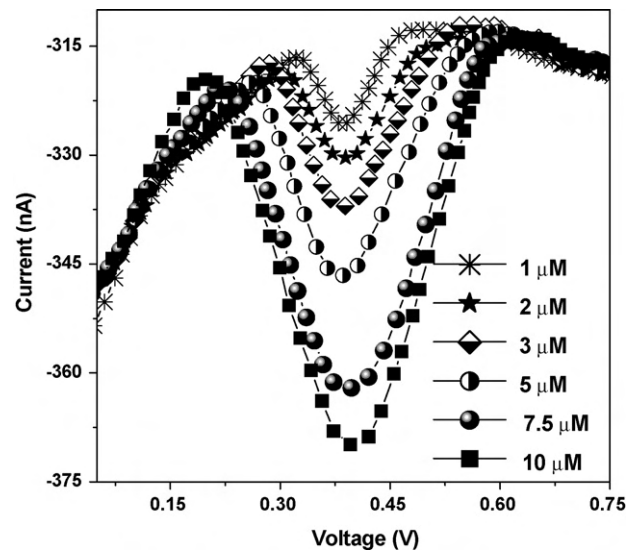


Fig. 4. Voltammograms of dopamine at different concentration using TiN (200)/NiTi as working electrode.

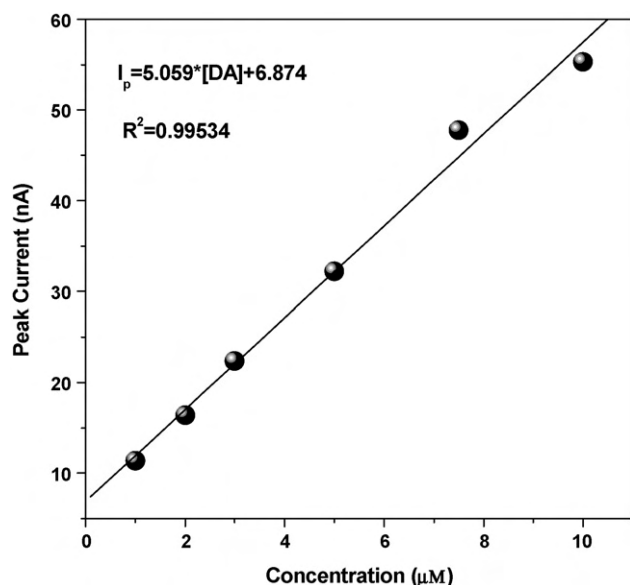


Fig. 5. Observed dependence of peak current on concentration of dopamine at TiN (200)/NiTi working electrode at pH 7.2.

abundantly present in biological samples. Hence, the effect of these two common interferents, which may interfere with determination of dopamine in blood or urine samples was also studied using TiN (200)/NiTi coated silicon electrode. It was found that ascorbic acid and uric acid showed well-defined peaks at modified electrode with  $E_p \sim 608$  and  $812$  mV vs. Ag/AgCl, respectively at pH 7.2. To check the interference of these two compounds, voltammograms were recorded at fixed concentration of dopamine ( $5 \mu\text{M}$ ) with varying concentration of ascorbic acid and uric acid. It was found that peak current of dopamine remained practically unaffected when ascorbic acid and uric acid were added in the concentration range  $50$ – $500 \mu\text{M}$  as shown in Table 2.

On the basis of the observations presented in Table 2, it can be concluded that ascorbic acid and uric acid do not interfere with voltammetric determination of dopamine even when they are in 100-fold excess with respect to dopamine. However, further increase in concentration of ascorbic acid beyond 100 times excess, causes a tendency to merge oxidation peak of ascorbic acid with oxidation peak of dopamine.

### 3.3.3. Stability of modified electrode

Stability and reproducibility of an electrode are the two important features which should be evaluated for analytical purpose. TiN (111)/NiTi and TiN (200)/NiTi coated silicon electrodes were tested for both the features so that a time period can be recommended for assured and accurate use of modified electrode. The variation in current response was observed for six successive

Table 2  
Effect of interferents on peak current of  $5 \mu\text{M}$  dopamine at pH 7.2.

| Interferent   | Concentration of interferents ( $\mu\text{M}$ ) | Peak current ( $i_p$ ) of dopamine ( $\mu\text{A}$ ) | Change in $i_p$ of dopamine |     |
|---------------|---|--|-----------------------------|-----|
|               |   |  | ( $\mu\text{A}$ )           | (%) |
| Ascorbic acid | 50  | 0.351  | +0.005                      | 1.4 |
|               | 125   | 0.353  | +0.007                      | 2.1 |
|               | 250   | 0.356  | +0.010                      | 2.8 |
|               | 500   | 0.363  | +0.017                      | 4.9 |
| Uric acid     | 50  | 0.349  | +0.003                      | 1.1 |
|               | 125   | 0.341  | -0.005                      | 1.4 |
|               | 250   | 0.355  | +0.009                      | 2.6 |
|               | 500   | 0.360  | +0.014                      | 4.2 |

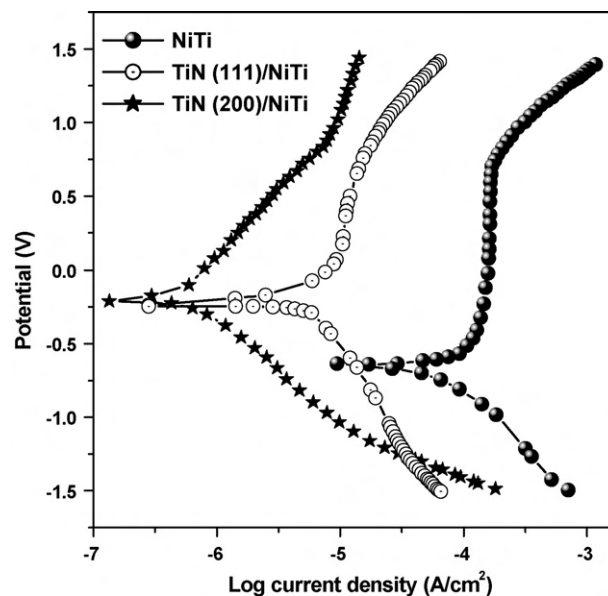


Fig. 6. Potentiodynamic polarization curves of NiTi, TiN (111)/NiTi and TiN (200)/NiTi films.

sweeps in a solution of fixed concentration to check the reproducibility of the electrode. It was noticed that the current was within 97–99% of the  $i_p$  observed for the first sweep. To determine long-term stability of TiN/NiTi coated silicon electrode, current response of dopamine was monitored daily for one week. The electrode was kept in dry conditions after use and it was found that the electrode retained 96–99% current for first three days. After three days, a considerable decline in the peak current was observed and only 91–95% of initial  $i_p$  was recorded. Thus, the electrode can be used for approximately three days without any significant error.

### 3.3.4. Corrosion resistance

Potentiodynamic polarization curves of NiTi, TiN (111)/NiTi and TiN (200)/NiTi films are shown in Fig. 6. The corrosion resistance of TiN coated NiTi films was found to be improved, which can be observed by a shift of whole polarization curve towards the region of lower current density and higher potential. The values of corrosion potential and corrosion current density were found to be  $0.635$  V and  $1.1 \times 10^{-5} \text{ A cm}^{-2}$  for pure NiTi film,  $0.248$  V and  $2.8 \times 10^{-7} \text{ A cm}^{-2}$  for TiN (111)/NiTi film and  $0.212$  V and  $1.4 \times 10^{-7} \text{ A cm}^{-2}$  for TiN (200)/NiTi film, respectively. High corrosion potential and low corrosion current density of the TiN coated NiTi films suggests that these films exhibit a low corrosion rate and a good corrosion resistance. TiN (200)/NiTi film exhibited better corrosion resistance than that of TiN (111)/NiTi film, which could be due to the fact that TiN (200) coated film exhibit higher real surface area/projected area and lower inhomogeneous surface. The real surface area is likely to be in the order, TiN (200)/NiTi > TiN (111)/NiTi > NiTi because, the grain size of these films follow the trend like TiN (200)/NiTi < TiN (111)/NiTi < NiTi. Therefore, smaller the grain size, higher will be the real surface area. The lower surface area and inhomogeneities might be responsible for weak points on the surface cause corrosive attacks.

## 4. Conclusions

A systematic study was performed to see the influence of crystallographic orientation of TiN passivation layer on mechanical and corrosion properties of NiTi thin films. The preferred orientation of the TiN films was observed to change from (111) to (200) with change in nature of sputtering gas. The shape of the crystallite

was also observed to change from a faceted pyramid to nonfaceted spherelike structure with change in crystallographic orientation of nanocrystalline TiN from (1 1 1) to (2 0 0). Nanoindentation studies revealed that the TiN (2 0 0)/NiTi films exhibit high hardness, high reduced elastic modulus and thereby better wear resistance as compared to pure NiTi and TiN (1 1 1)/NiTi. Electrochemical test reveals that TiN coated NiTi film exhibited better corrosion resistance as compared to pure NiTi film. It was also observed that TiN (2 0 0)/NiTi coated silicon electrode showed better response as compared with NiTi coated silicon with straight line calibration in dopamine concentration range 1–10  $\mu$ M. One of the probable reasons for this observation is that as TiN (2 0 0)/NiTi film exhibits higher real surface area due to small grain size as compared to NiTi film, TiN (2 0 0)/NiTi film showed better oxidation peak even at low concentration of dopamine. A significant decrease in peak potential was also observed at modified electrode. An advantage of using these nanocrystalline films in comparison to conventional films used for surface modification is that the films are sufficiently stable and do not require frequent replacements. Such replacement not only requires sufficient time but may also lead to change in the area of the electrode. In addition the films exhibit excellent electrocatalytic behaviour. Thus, it is concluded that use of nanocrystalline TiN layer with preferred (2 0 0) orientation on NiTi thin films improves mechanical, corrosion and electrocatalytic properties and hence can be successfully used as working electrode in voltammetric determination of biomolecules.

#### Acknowledgements

Financial support for carrying out this work was provided by Ministry of Communications and Information Technology, DIT, New Delhi vide grant No. 20(II)/2007-NANO under nanotechnology initiatives scheme. One of the authors (AK) is thankful to DIT for Senior Research Fellowship and to Dr. Sudhanshu P. Singh, Senior Research

Fellow, Department of Chemistry, IIT Roorkee for his help in electrochemical studies. Authors are thankful to Prof. A.K. Raychaudhary, SNBNCBS, India and Prof. Jan. Humbuck, Leuven University, Belgium for helpful discussions.

#### References

- [1] D. Xu, L. Wang, G. Ding, Y. Zhou, A. Yu, B. Cai, *Sens. Actuators A: Phys.* 93 (2001) 87.
- [2] B. O'Brien, W.M. Carroll, M.J. Kelly, *Biomaterials* 231 (2002) 739.
- [3] J.J. Gill, D.T. Chang, L.A. Momoda, G.P. Carman, *Sens. Actuators A: Phys.* 93 (2001) 148.
- [4] G.C. McKay, R. Macnair, C. MacDonald, M.H. Grant, *Biomaterials* 17 (1996) 1339.
- [5] D.J. Wever, A.G. Veldhuizen, J. Vries de, H.J. Busscher, J.R. van Horn, *Biomaterials* 19 (1998) 761.
- [6] X. Zhao, W. Cai, L. Zhao, *Surf. Coat. Technol.* 155 (2002) 236.
- [7] Z.D. Cui, H.C. Man, X.J. Yang, *Surf. Coat. Technol.* 192 (2005) 347.
- [8] G.S. Firstov, R.G. Vitchev, H. Kumar, B. Blanpain, J. Van, *Biomaterials* 23 (2002) 4863.
- [9] P. Shi, F.T. Cheng, H.C. Man, *Mater. Lett.* 61 (2007) 2385.
- [10] P. Singh, D. Kaur, *J. Appl. Phys.* 103 (2008) 043507.
- [11] R. Chandra, D. Kaur, A.K. Chawla, N. Phinichka, Z.H. Barber, *Mater. Sci. Eng. A* 423 (2006) 111.
- [12] S.A. Shabalovskaya, *Bio-Med. Mater. Eng.* 12 (2002) 69.
- [13] A. Thompson, *Int. Endo. J.* 33 (2000) 297.
- [14] R.N. Goyal, N. Bachheti, A. Tyagi, A.K. Pandey, *Anal. Chim. Acta* 605 (2007) 34.
- [15] R.N. Goyal, M. Oyama, S.P. Singh, *J. Electroanal. Chem.* 611 (2007) 140.
- [16] Y. Tao, Z. Lin, X. Chen, X. Huang, M. Oyama, X. Chen, X. Wang, *Sens. Actuators B: Chem.* 129 (2008) 758.
- [17] R.N. Goyal, V.K. Gupta, S. Chatterjee, *Talanta* 76 (2008) 662.
- [18] J. Zhang, M. Oyama, *J. Electroanal. Chem.* 577 (2005) 273.
- [19] R.N. Goyal, S.P. Singh, *Carbon* 46 (2008) 1556.
- [20] R.N. Goyal, V.K. Gupta, M. Oyama, N. Bachheti, *Talanta* 72 (2007) 976.
- [21] T.M. Dawson, *Science* 302 (2003) 819.
- [22] M.C. Shih, M.Q. Hoexter, L.A.F. Andrade, *Revista Paulista de Medicina* 124 (2006) 168.
- [23] G.D. Christian, W.C. Purdy, *J. Electroanal. Chem.* 3 (1962) 363.
- [24] W. Ni, Y.T. Cheng, D.S. Grummon, *Appl. Phys. Lett.* 82 (2003) 2811.
- [25] W. Ni, Y.T. Cheng, M.J. Lukitsch, A.M. Weiner, L.C. Lev, D.S. Grummon, *Appl. Phys. Lett.* 85 (2004) 4028.